Dalton Transactions

PAPER

View Article Online
View Journal | View Issue

Cite this: *Dalton Trans.*, 2015, **44**, 14763

An effective combination of electrodeposition and layer-by-layer assembly to construct composite films with luminescence switching behavior†

Wenmei Gao,[a] Hongwei Ma,[a] Daming Zheng,[a] Zhaojun Dong,[b] Lixin Wu[a] and Lihua Bi*[a]

Received 30th May 2015,
Accepted 13th July 2015

DOI: 10.1039/c5dt02051d

www.rsc.org/dalton

This article presents a combination strategy of electrodeposition and a layer-by-layer assembly to fabricate functional composite films with luminescence switching behavior. Firstly, a novel green luminescence film consisting of 8-hydroxypyrene-1,3,6-trisulfonic acid trisodium salt (HOPTS) was first obtained on ITO by a facile electrodeposition method. Then, the multilayer films containing different layers of tungstophosphate $K_{12.5}Na_{1.5}[NaP_5W_{30}O_{110}]\cdot 15H_2O$ (P_5W_{30}) were further fabricated on the green luminescence film to form the composite films [$(HOPTS)_{50}/(PDDA/P_5W_{30})_n$] ($n$ = 10, film 1; n = 27, film 2; n = 57, film 3). Cyclic voltammetry and fluorescence spectroscopy were used to characterize the electrochemical activity of P_5W_{30} and the luminescence property of HOPTS in the composite films, respectively. Lastly, *in situ* UV-Vis spectroelectrochemical and fluorescence spectroelectrochemical measurements were applied to investigate the luminescence switching behaviors of the composite films controlled by the electrochromism component of P_5W_{30} upon electrochemical modulation. In summary, the investigation results revealed that the electrodeposition method is convenient and rapid, and thus-prepared composite films showed improved luminescence switching performance in terms of switching process, activation cycles, coloration efficiency, and bleached-state transparency as well as good stability, wide voltage range and good reversibility. Therefore, the present study offers a new fabrication route for the multifunctional composite films through an effective combination of electrodeposition and layer-by-layer assembly technique.

Introduction

Polyoxometalates (POMs) represent a well-known class of inorganic metal–oxide nanoclusters with intriguing structures and diverse chemical and electrical properties,[1–5] which have been applied in many fields such as catalysis,[6] nanotechnology,[7] and materials science.[8] According to the literature reports, the advantages of POMs are as follows: POMs can undergo reversible and stepwise multielectron-transfer reactions while retaining their structural integrity;[9] most of the POMs show high solubility in water, which is easy for the construction of the materials, especially, the properties of POMs can be retained very well in the materials;[10] some POMs can accept electrons to form the reduced POMs, giving rise to the deep-blue colored mixed-valence state species, which exhibit a broad absorption band in the range of 400 nm–800 nm;[11] the structures of POMs can be tailored *via* changing the composition of the building blocks to obtain the ability of reserving different electrons and result in adjustable electrical properties;[12] the properties of POM-based materials can be modulated by an external stimulus including UV/Vis light irradiation,[13] electrochemical stimulation,[14] and acid–base gases.[15] Consequently, these advantages of POMs make them become one of the most promising candidates for the construction of functional materials.

The functional materials with luminescence switching behaviors are being developed for applications in sensors,[16] optical and electronic devices,[17] fluorescence imaging,[18] and displays.[19] These materials are normally composed of fluorescence and stimuli-response components together, and the switching of luminescence could be manipulated reversibly by different types of external triggers, such as thermal,[20] electri-

[a]*College of Chemistry, State Key Laboratory of Supramolecular Structure and Materials, Jilin University, Changchun 130012, P. R. China.*
E-mail: blhytyyz@163.com; Fax: +86 431 85193421; Tel: +86 431 85168499
[b]*Key Lab of Groundwater Resources and Environment Ministry of Education, College of Environment and Resources, Jilin University, Changchun 130021, P. R. China*

†Electronic supplementary information (ESI) available: CVs of HOPTS and P_5W_{30} in solutions; electrodeposition CVs at different potential ranges; AFM images of the films $(HOPTS)_m$; UV-Visible dynamic and chronoamperometry curves of three composite films; luminescence spectra of the film $(HOPTS)_{50}$ and roughness of different HOPTS films. See DOI: 10.1039/c5dt02051d

cal,[21] optical,[22] and/or chemical stimulus.[23] On account of the above mentioned advantages of POMs, in recent years, POM-based reversible fluorescent switchable materials are explored and several samples have been reported,[24,25] in which the luminescence switching was realized *via* a fluorescence resonance energy transfer (FRET) between the reduced POM component and luminescence species.[26] Due to the energy-efficient, environmentally-friendly and ultrafast power source of the electrochemical technique, we firstly used it as an external stimulus to control the luminescence switching of POM-based luminescence composite films.[27] Moreover, the investigation reveals that the reduced POM exhibits a broad absorption band in the visible range covering the green and red light regions, suggesting that the POMs can switch not only red fluorescence but also green fluorescence. Recently, we firstly developed a green luminescence composite film, taking fluorescein as a green luminescence molecule. Unfortunately, it could not be directly fabricated onto the composite film with POM by a layer-by-layer (LBL) assembly method due to the structure feature and low charge of fluorescein (FL), but instead, FL was firstly loaded on the surface of graphene oxide (GO) to form the hybrid GO–FL, and then the precursor GO–FL was further used to prepare the composite films $\{[(PEI/P_5W_{30})_m/(PEI/PSS/PEI/GO@F)]_n(PEI/P_5W_{30})_m\}$ (m = 1, 3, 5; n = 15, 17, 18).[28] However, the use of such a fabrication strategy is dramatically restricted by the drawbacks of the composite film including low on–off contrast, narrow voltage range and low luminescence switching efficiency due to the existence of brown GO. Therefore, the search for a new method to prepare POM-based green luminescence film is extremely urgent.

Herein we explore a new method of a simple and low cost process to fabricate stable green luminescence composite films by an effective combination of electrodeposition with a layer-by-layer assembly technique. On one hand, HOPTS not only exhibits the yellow green luminescence but also possesses the functional group for polymerization (see Scheme 1). Moreover, the HOPTS-based polymerized film can maintain its yellow green luminescence behavior. So HOPTS was selected as the green luminescence active component; on the other hand, the redox behaviors of P_5W_{30} were investigated clearly in solution and can be fully maintained in the composite films. In addition, P_5W_{30} possesses high negative charge (−15) and large size (2 nm), which can be adsorbed more easily by the oppositely charged species onto the composite films (see Scheme 1). Therefore, P_5W_{30} was chosen as the electro-active species. Thus-prepared composite films containing HOPTS and P_5W_{30} display a relatively high on–off contrast, good reversibility, excellent stability, wide voltage range and high luminescence switching efficiency.

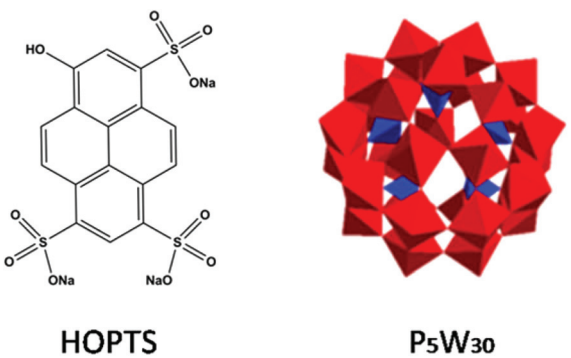

Scheme 1 The molecular structure of HOPTS (left) and polyhedral representation of P_5W_{30} (right). The WO_6 octahedra are shown in red and the PO_4 tetrahedra are shown in blue.

Experimental section

Materials

The tungstophosphate $K_{12.5}Na_{1.5}[NaP_5W_{30}O_{110}]\cdot 15H_2O$ (P_5W_{30}) was prepared according to the literature method and identified by IR spectroscopy, UV spectroscopy and cyclic voltammetry.[29] HOPTS and poly(diallyldimethylammonium chloride) (PDDA, MW 100 000–200 000) were purchased from Sigma-Aldrich and used without further purification. Other related chemicals are of analytical grade. Water was purified using a Millipore Millip-Q water purification system. 0.5 M H_2SO_4/Na_2SO_4 solution (pH = 2.5) was used as the electrolyte solution throughout the experiments.

Instruments

UV-Vis absorption spectra were collected with a Varian Cary 50 UV-Vis spectrophotometer. A FLS980 spectrofluorometer was employed to detect the fluorescence emission spectra. All the electrochemical experiments were carried out on a CHI 660C electrochemical workstation. A three-electrode system was used for the whole electrochemical experiment in a quartz cell or an electrolytic cup with a reference electrode (Ag/AgCl), a counter electrode (a platinum foil) and a working electrode (blank ITO or ITO modified by the composite films). Electrochromic measurements were performed by using an *in situ* spectroelectrochemical system which combined a CHI 660C electrochemical workstation and a Varian Cary 50 UV-Vis spectrophotometer. Electroswitchable luminescence response experiments were carried out through an *in situ* fluorescence spectroelectrochemical system which combined a CHI 660C electrochemical workstation and an FLS980 spectrofluorometer. Atomic force microscopy (AFM) measurements were performed in air with a SPA 400 instrument.

Preparation of HOPTS film

The electrodeposition method was employed to prepare the HOPTS film on the ITO surface. 10 mg HOPTS was dissolved in 10 mL 0.5 M H_2SO_4/Na_2SO_4 (pH = 2.5) solution, and then the HOPTS was electropolymerized directly onto the ITO electrodes *via* repeated scanning between −1.0 and +1.0 V in certain cycles. The electrodeposited HOPTS film modified ITO electrode was washed by deionized water several times and then dried under a nitrogen flow. The thickness of the HOPTS film can be controlled by the choice of scanning cycles.

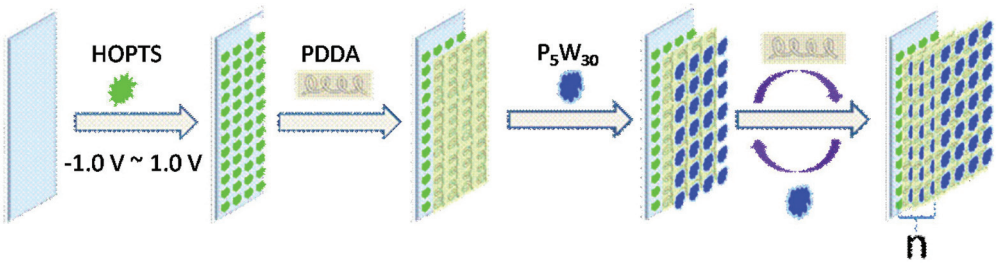

Fig. 1 Schematic of the composite film $[(HOPTS)_{50}/(PDDA/P_5W_{30})_n]$.

Fabrication of the composite film $[(HOPTS)_{50}/(PDDA/P_5W_{30})_n]$

The above HOPTS film modified ITO electrodes were dipped into freshly prepared 10 mg mL^{-1} PDDA and 2 mM P_5W_{30} aqueous solutions for 20 minutes respectively, followed by washing with deionized water and drying under a nitrogen flow. This process can be repeated many times to obtain the composite films with different layers of electrochromic component P_5W_{30}. The above procedure promoted the build-up of composite films containing HOPTS-based electrodeposited film and POMs, which can be expressed as $[(HOPTS)_{50}/(PDDA/P_5W_{30})_n]$ (n = 10, 27, 57), where 50 stands for the scanning cycle numbers between +1.0 V and −1.0 V during the electropolymerization process of HOPTS and n represents the layer number of $(PDDA/P_5W_{30})$ in the process of layer-by-layer self-assembly. The fabrication process of composite films is schematically illustrated in Fig. 1.

Results and discussion

The property studies of P_5W_{30} and HOPTS in solutions

It has been reported that the oxidized form of P_5W_{30} is colorless and fully transparent without apparent absorption in the whole visible region of 400–800 nm (see Fig. 2, black curve) while the reduced form of P_5W_{30} is dark blue and exhibits a broad absorption feature in the visible region, originating from the $W^{5+} \rightarrow W^{6+}$ intervalence charge-transfer (IVCT) (see Fig. 2, blue curve), and the reduced P_5W_{30} can be oxidized with a suitable oxidation potential to recover its original colorless state.[28] Meanwhile, the characteristic emission of HOPTS in solution is at about 512 nm as shown in Fig. 2 (green curve). It can be seen from Fig. 2 that the absorption band of electro-reduced P_5W_{30} exhibits a relatively favorable overlap with the luminescence spectrum of HOPTS, meaning that the highly efficient energy transfer between luminescent species HOPTS and electro-reduced P_5W_{30} should happen if both HOPTS and P_5W_{30} are in the same composite film. Therefore, it is expected that P_5W_{30} can be used as a partner of HOPTS to reversibly switch luminescence of HOPTS through the redox process of P_5W_{30} under electrochemical stimulation.

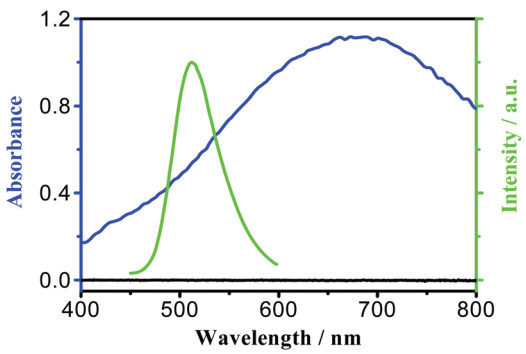

Fig. 2 UV-Vis spectra of P_5W_{30} in its initial state (black curve) and electro-reduced state (blue curve), and normalized luminescence spectrum of HOPTS (green curve) in 0.5 M H_2SO_4/Na_2SO_4 (pH = 2.5) aqueous solutions.

Based on the above anticipation, we adopted a combination method of the electrodeposition and the layer-by-layer assembly technique to fabricate a series of composite films with different contents of P_5W_{30} for comparison purpose, and investigated their electrochromic and electrofluorochromic properties in detail.

The preparation and characterization of HOPTS film

The cyclic voltammogram (CV) of HOPTS in 0.5 M Na_2SO_4/H_2SO_4 (pH = 2.5) is shown in Fig. S1.† It can be seen that the HOPTS was oxidized at about −0.5 V. Based on different electropolymerization potentials (Fig. S2†), the potential range of 1.0 to −1.0 V was detected to be an optimal choice for the electrodeposition of the HOPTS film on the ITO substrate. Fig. 3 shows CVs of HOPTS with ten scanning cycles, in which the peak current gradually increases along with the potential scanning repeatedly, indicating the uniform growth of electrodeposition of HOPTS and the formation of a coating on the electrode surface due to the formation of crosslinking between HOPTS which is similar to the electropolymerization process of pyrene.[30] Atomic force microscopy (AFM) measurement further characterizes the surface morphology of the HOPTS film on ITO (see Fig. 4), which displays cross-linked cone microspheres of the $(HOPTS)_{50}$ film with the particle size of about 100 nm and the root mean square (RMS) of 3.481 nm. For comparison, we prepared the HOPTS film with different scanning cycles of $(HOPTS)_{10}$ and $(HOPTS)_{27}$, and characterized their surface morphologies as shown in Fig. S3 and S4.† The computed surface roughness of three HOPTS films is

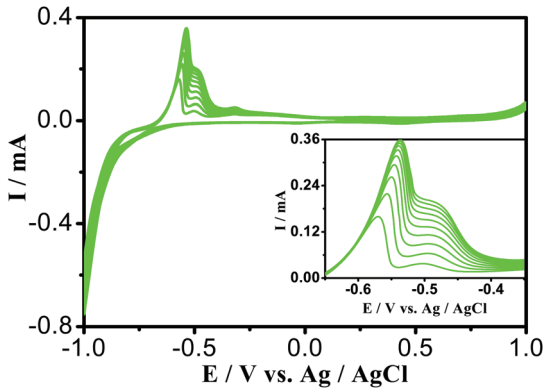

Fig. 3 Electrodeposition process of $(HOPTS)_m$ film on ITO electrode from −1.0 V to 1.0 V at a scan rate of 100 mV s^{-1} in 10 mL 0.5 M H_2SO_4/Na_2SO_4 solution (pH = 2.5) containing 0.02 mmol HOPTS.

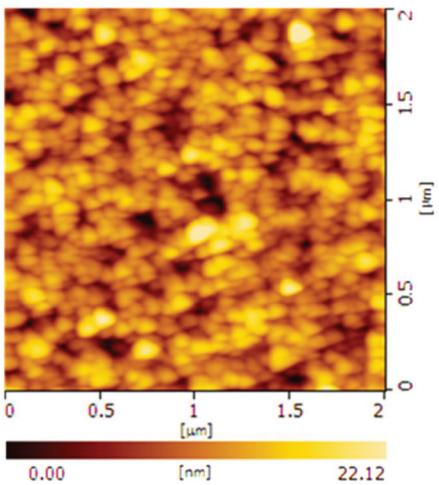

Fig. 4 AFM image of $(HOPTS)_{50}$ film on ITO substrate in the scanning range of 2 micrometers.

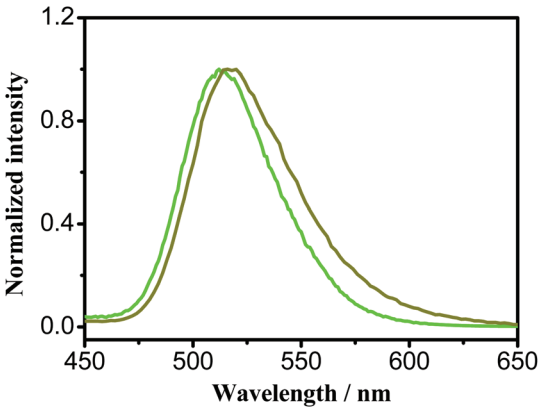

Fig. 5 Normalized luminescence spectra of HOPTS (green curve) in 0.5 M H_2SO_4/Na_2SO_4 (pH = 2.5) aqueous solution and HOPTS film (dark yellow curve).

listed in Table S1,† which exhibits the RMS values increased with the scanning cycles, further confirming the formation of the HOPTS film on ITO.

Encouragingly, the luminescence performance of HOPTS is still maintained in the HOPTS film, as shown in Fig. 5. Compared with free HOPTS in solution, which showed a characteristic emission at around 512 nm, the luminescence spectrum of the HOPTS film is not substantially altered, except for a small red shift in the luminescence maximum of HOPTS. Such a bathochromic shift in the luminescence peak may be due to FRET of the aggregated HOPTS in the same film, originating from a structural change of the luminescence molecule and the π–π stacking interaction in the HOPTS film.

The preparation and characterization of the composite films $[(HOPTS)_{50}/(PDDA/P_5W_{30})_n]$

Based on the above deposited HOPTS film, the positively-charged PDDA was selected as molecular linkers to gradually integrate the negatively-charged P_5W_{30} into the composite films on ITO electrodes. For comparison purpose, five composite films $[(HOPTS)_{50}/(PDDA/P_5W_{30})_n]$ (n = 5, 10, 20, 27, 57) with different layers of P_5W_{30} were prepared by a combination of electrodeposition with a layer-by-layer assembly technique. Five composite films are verified to be uniformly assembled by their CV curves (see Fig. 7) and visible absorption spectra upon the application of a negative potential (see Fig. 8). Fig. 6 shows the absorbance in visible absorption spectra of the composite films at the applied potential of −0.7 V and the first anodic oxidation peak currents of the composite films as the function of the number of layers. It is clearly shown that as the number of layers increases, two linear increases are observed in the absorbance and current, demonstrating a nearly uniform growth of three composite films. Moreover, the absorbance and current are in proportion to the content of P_5W_{30} in

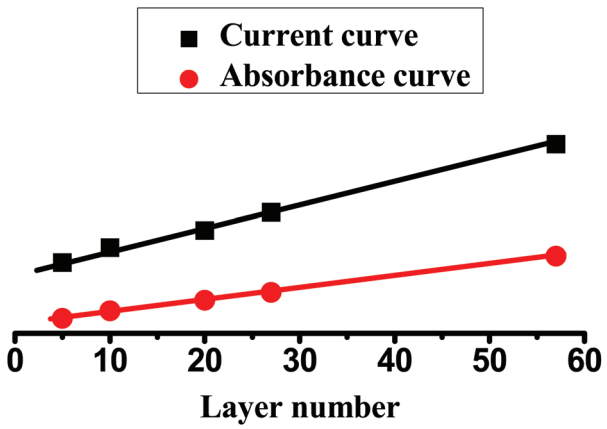

Fig. 6 The relationship of the maximum absorbance in visible absorption spectra at the applied potential of −0.7 V and first anodic oxidation peak current of five composite films with the number of layers in $[(HOPTS)_{50}/(PDDA/P_5W_{30})_n]$ (n = 5, 10, 20, 27, 57).

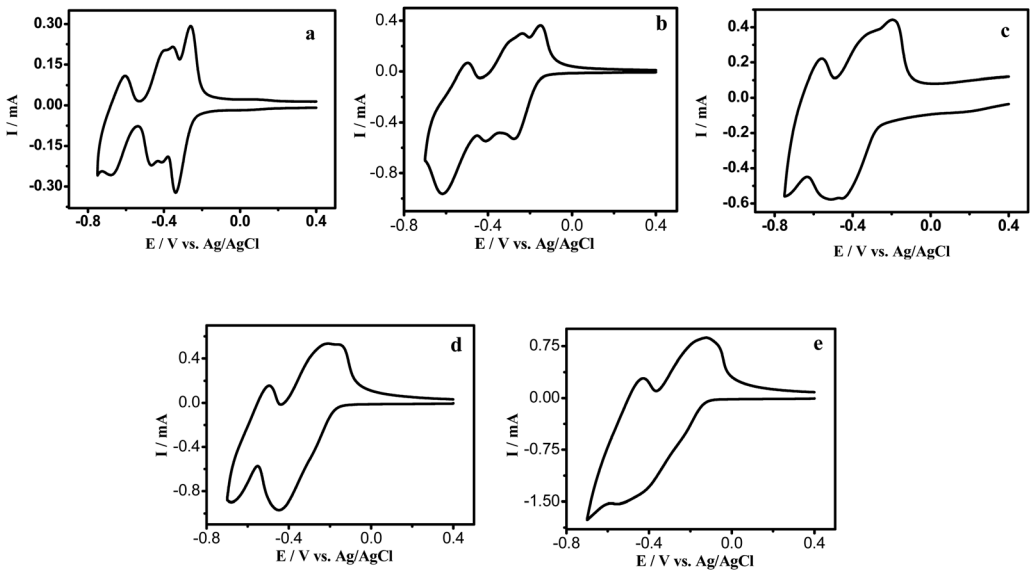

Fig. 7 CVs of three composite films in 0.5 M H_2SO_4/Na_2SO_4 (pH = 2.5) with a scan rate of 100 mV s^{-1}: (a) $[(HOPTS)_{50}/(PDDA/P_5W_{30})_5]$; (b) $[(HOPTS)_{50}/(PDDA/P_5W_{30})_{10}]$; (c) $[(HOPTS)_{50}/(PDDA/P_5W_{30})_{20}]$; (d) $[(HOPTS)_{50}/(PDDA/P_5W_{30})_{27}]$; (e) $[(HOPTS)_{50}/(PDDA/P_5W_{30})_{57}]$.

the composite films, indicating that the performance of the composite films can be controlled by the layers of P_5W_{30}.

As shown in Fig. 7, it can be seen that the CV curves in Fig. 7a and b are similar, the CV curves in Fig. 7c–e are similar, whereas the CVs in Fig. 7a and b are little different from that in Fig. 7c–e. The little difference between them is ascribed to the composite films with different layer numbers of P_5W_{30}.

When the layer numbers of the composite films are less than 10, the P_5W_{30} species are close to the electrode and the content of PDDA is lower in the composite films, the rate of electron transfer from electrode to P_5W_{30} is faster. As a result, three couples of redox waves for P_5W_{30} in the composite films $[(HOPTS)_{50}/(PDDA/P_5W_{30})_n]$ (n = 5 and 10) can be clearly separated. When the layer numbers of the composite films are more than 10, some P_5W_{30} species are far from the electrode and the content of PDDA and the interaction of P_5W_{30} with PDDA are increased in the composite films, which would block the electron transfer although PDDA is conductive polymer, resulting in the decrease of the rate of electron transfer from electrode to P_5W_{30}. On the one hand, the decrease of the rate of electron transfer induced the shifts in the formal potential and increase in the peak to peak potential separations with layer numbers; on the other hand, the decrease of the rate of electron transfer resulted in overlapping of the first and second couples of redox waves, which can be confirmed by broader redox waves in Fig. 7c–e.

As a consequence, five composite films exhibit similar redox behaviors compared with P_5W_{30} in solution (see Fig. S5†), confirming that electrochemical activity of P_5W_{30} is fully maintained in the composite films. Moreover, the good linear correlation shown in Fig. 6 further affirms the above conclusion because PDDA species do not exhibit any redox waves in the same potential range on the ITO electrode during the LBL assembly process.

Electrochromism properties, stability and reversibility studies of three composite films

The electrochromic properties of three composite films were further examined by recording the absorption spectra at different applied potentials. As shown in Fig. 8, the more negative the applied potentials, the higher the absorbance appeared in the visible region, while there is no apparent absorption in the visible region under open circuit (black line), confirming the increase of the electro-reduced P_5W_{30} in the composite films with a reduction degree. Accordingly, it is expected that the energy transfer efficiency between P_5W_{30} and HOPTS can be regulated by applying different potentials.

The stability and reversibility of the composite films were investigated to make sure that the as-prepared composite films possess potential applications as functional materials. After UV-Vis dynamic curves of absorbance at 650 nm and chronoamperometry curves of three composite films are measured under the same experimental conditions, it can be seen that the response times for coloration and bleaching as well as the absorbance of the electrochromic window and curves of the redox currents for all three composite films do not show noticeable change after 40 cycles (see Fig. S6 and S7†). The above observation demonstrates the stable electrochromic behaviors and good reproducibility of the optical responses for three composite films under their optimum redox potential ranges.

Electrofluorochromic properties, stability and reversibility studies of three composite films

For comparison, the luminescence spectra of $(HOPTS)_{50}$ in its oxidation and reduction states were recorded in order to

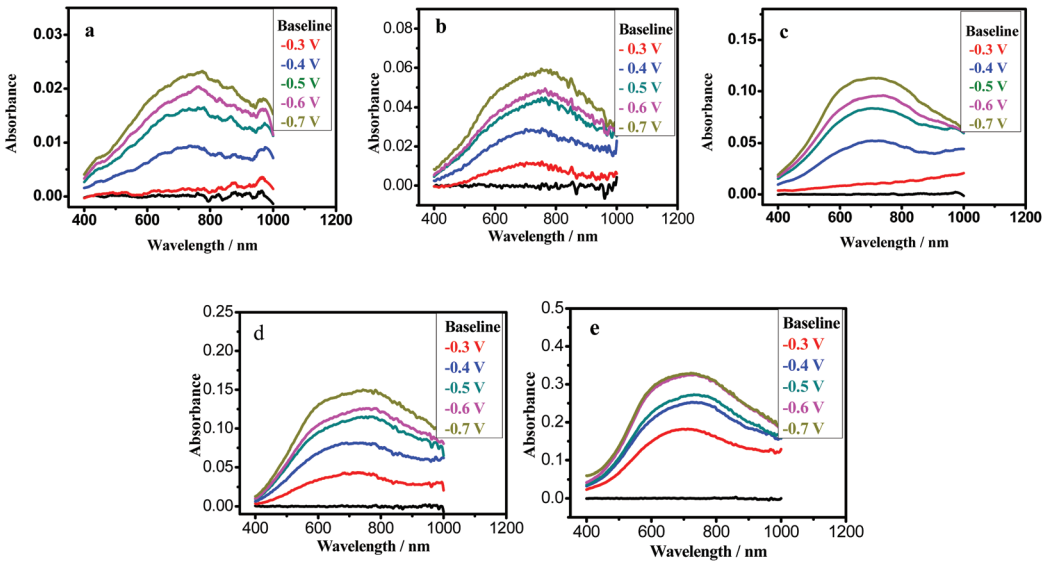

Fig. 8 UV-Vis spectra of three composite films in 0.5 M Na_2SO_4/H_2SO_4 (pH = 2.5) solutions upon the application of different reduction potentials for 1 min: (a) $[(HOPTS)_{50}/(PDDA/P_5W_{30})_5]$; (b) $[(HOPTS)_{50}/(PDDA/P_5W_{30})_{10}]$; (c) $[(HOPTS)_{50}/(PDDA/P_5W_{30})_{20}]$; (d) $[(HOPTS)_{50}/(PDDA/P_5W_{30})_{27}]$; (e) $[(HOPTS)_{50}/(PDDA/P_5W_{30})_{57}]$.

examine the influence of reduction potential on luminescence intensity (see Fig. S8†). It is noteworthy that the luminescence spectrum at the potential of −0.7 V does not cause either the shift of the peak position or alteration of the peak shape, meaning that the luminescence performance of the film $(HOPTS)_{50}$ is stable during the redox process. Subsequently, we determined the luminescence spectra of three composite films at different applied potentials. As shown in Fig. 9, it can be observed that the luminescence quenching degree of the composite films increases with the increase of the reduced potentials. The above results of the contrast experiments indicate unambiguously that the electrofluorochromic performance of three composite films is attributed to the energy transfer from luminescence species HOPTS to electro-reduced P_5W_{30}. These results are consistent with the above anticipation.

The fluorescence switching response of three composite films was investigated during the potential cycles between +0.7 V and −0.7 V many times for clear comparison. As shown in Fig. 10, in open circuit, three composite films could emit their characteristic luminescence bands of HOPTS (black curves), while luminescence intensities of three composite films were all decreased in different degrees upon the application of a reduction potential of −0.7 V (blue curve). After an oxidation potential of 0.7 V was further applied, the luminescence intensities were recovered to their initial states (green curve). Moreover, the "on" and "off" states of the luminescence switching was basically reversible and can be repeated several times without distinct changes in luminescence intensity after many cycles of double-potential steps, displaying excellent cycling performance. Further, in order to represent the efficiency of luminescence quenching quantitatively, we calculated the normalized integral areas of luminescence spectra (insets in Fig. 10). As expected, the luminescence quenching efficiencies of three composite films are differently attributed to the different contents of P_5W_{30} in the three composite films, that is, the efficiencies of luminescence quenching are calculated

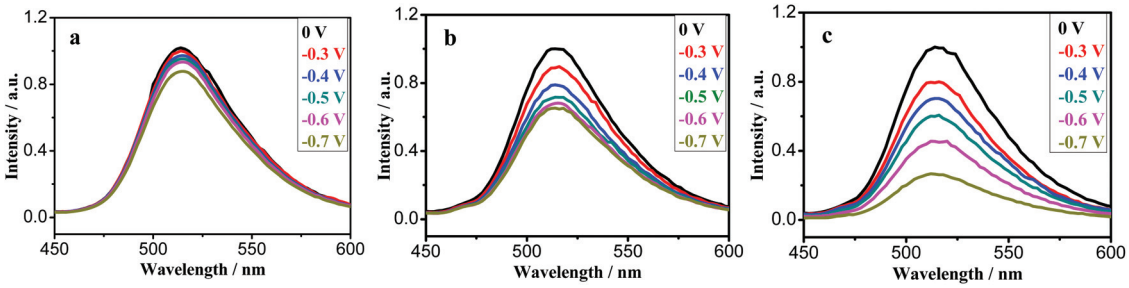

Fig. 9 Normalized luminescence spectra of three composite films in 0.5 M Na_2SO_4/H_2SO_4 (pH = 2.5) solutions when different reduction potentials were applied for 1 minute: (a) $[(HOPTS)_{50}/(PDDA/P_5W_{30})_{10}]$; (b) $[(HOPTS)_{50}/(PDDA/P_5W_{30})_{27}]$; (c) $[(HOPTS)_{50}/(PDDA/P_5W_{30})_{57}]$.

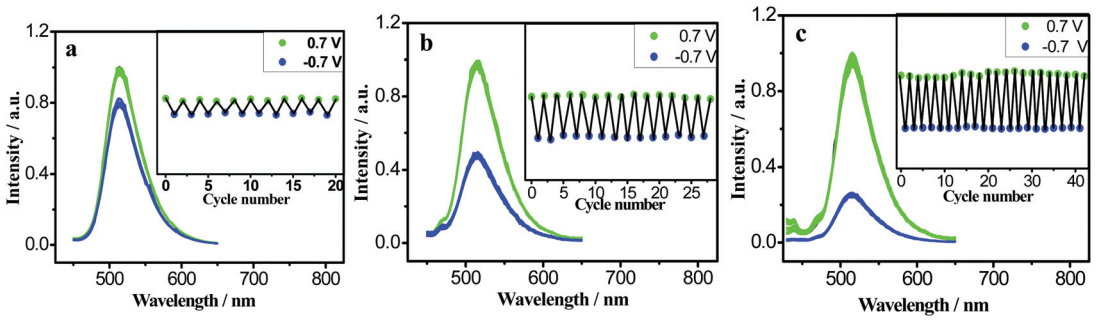

Fig. 10 Normalized fluorescence switching of three composite films in 0.5 M Na_2SO_4/H_2SO_4 (pH = 2.5) solutions and normalized fluorescence integral area (insets) as a function of cycle number in double-potential cycles. Composite films from open circuit (black curve), to a negative potential and a positive potential. Blue curves and dots were measured after composite films were reduced at an negative potential of −0.7 V for 1 minute, and green curves and dots were collected after composite films were oxidized at an positive potential of 0.7 V for 1 minute: (a) $[(HOPTS)_{50}/(PDDA/P_5W_{30})_{10}]$; (b) $[(HOPTS)_{50}/(PDDA/P_5W_{30})_{27}]$; (c) $[(HOPTS)_{50}/(PDDA/P_5W_{30})_{57}]$.

Table 1 Comparison of the luminescence performance of different composite films

	Film 1	Film 2	Film 3	Film 4	Film 5	Film 6
Ratio of POM layers and luminescence species layer	10 : 50 ≈ 0.2	27 : 50 ≈ 0.54	57 : 50 ≈ 1.14	16 : 15 ≈ 1.07	54 : 17 ≈ 3.18	95 : 18 ≈ 5.28
Luminescence quenching efficiency	20%	48%	75%	11%	51%	88%
Applied potential range		−0.7 V to +0.7 V			−0.5 V to +0.5 V	

to be *ca.* 20% for film 1 (Fig. 10a), 48% for film 2 (Fig. 10b), and 75% for film 3 (Fig. 10c), which is in accordance with our initial design, that is, the on/off contrast of the composite films becomes higher with increasing the content of P_5W_{30}. Hence, it can be concluded that the fluorescence can be regulated by changing the content of P_5W_{30} in the composite films under identical conditions. This evidence is also in agreement with the mechanism that the luminescence-quenching is sourced from the intermolecular resonance energy transfer.

Compared with the composite films $\{[(PEI/P_5W_{30})_m/(PEI/PSS/PEI/GO@FL)]_n(PEI/P_5W_{30})_m\}$ (m = 1, n = 15, film 4; m = 3, n = 17, film 5; m = 5; n = 18, film 6) prepared by layer-by-layer assembly technology alone,[28] thus-prepared three composite films exhibit three typical features: (1) high luminescence quenching efficiency: the comparison for the content ratio of POM and luminescence species in the composite films and the luminescence performance of the composite films is listed in Table 1. It can be observed that the composite films 1–3 exhibit excellent luminescence quenching efficiencies although the ratio of the composite films 1–3 is lower than that of the composite films 4–6. (2) Wide applied potential range: as shown in Table 1, the repeated change in the luminescence quenching and recovery for the composite films 1–3 could be observed during the potential cycles of −0.7 V to +0.7 V compared to the composite films 4–6 in the potential range of −0.5 V to +0.5 V. (3) The simple and rapid fabrication process: this means that a longer time is needed to fabricate more layers of P_5W_{30} in the composite films 4–6 if the same luminescence quenching efficiency is needed. As a consequence, there is no doubt that the combination of electrodeposition with a layer-by-layer assembly technology is an effective strategy to prepare the multifunctional composite films.

Conclusions

In conclusion, we have demonstrated that the combination of electrodeposition with LBL assembly is an effective method to prepare the composite film consisting of a green luminescence species HOPTS and an electroactive component P_5W_{30}. Compared to the conventional LBL assembly alone, the synergistic strategy of the electrodeposition and LBL assembly is simple and rapid, and the current composite film displays high on/off contrast, good long-time stability and wide potential range. Furthermore, the luminescence intensity in the current system can be easily tuned by scanning cycles and fluorescence switching is realized by integrating different contents of P_5W_{30} into the same film. As a result, we believe that the methodology developed in this study could serve as a general approach to the development of other multifunctional composite films.

Acknowledgements

This research work was supported by the National Natural Science Foundation of China (21173102 and 21473072), the Technology of Jilin Province, China (20130101008JC).

References

1 (*a*) W. W. He, S. L. Li, H. Y. Zang, G. S. Yang, S. R. Zhang, Z. M. Su and Y. Q. Lan, *Coord. Chem. Rev.*, 2014, **279**, 141; (*b*) X. X. Li, W. H. Fang, J. W. Zhao and G. Y. Yang, *Chem – Eur. J.*, 2014, **20**, 17324.
2 M. Genovese and K. Lian, *Curr. Opin. Solid State Mater. Sci.*, 2015, **19**, 126.
3 S. Herrmann, C. Ritchie and C. Streb, *Dalton Trans.*, 2015, **44**, 7092.
4 D. L. Long, E. Burkholder and L. Cronin, *Chem. Soc. Rev.*, 2007, **36**, 105.
5 (*a*) R. X. Wang, Y. Li, K. Shetye, T. Dutta, L. Jin, S. H. Li and Z. H. Peng, *Eur. J. Inorg. Chem.*, 2015, **4**, 656; (*b*) T. Q. Wang, Z. X. Sun, F. Y. Li and L. Xu, *Electrochem. Commun.*, 2014, **47**, 45.
6 (*a*) I. N. Lykakis, E. Evgenidou and M. Orfanopoulos, *Curr. Org. Chem.*, 2012, **16**, 2400; (*b*) R. Q. Meng, L. Suo, G. F. Hou, J. Liang, L. H. Bi, H. L. Li and L. X. Wu, *CrystEngComm*, 2013, **15**, 5867; (*c*) X. L. Hao, Y. Y. Ma, H. Y. Zang, Y. H. Wang, Y. G. Li and E. B. Wang, *Chem. – Eur. J.*, 2015, **21**, 3778; (*d*) D. S. Gopala, R. R. Bhattacharjee and R. Richards, *Appl. Organomet. Chem.*, 2013, **27**, 1.
7 J. Lehmann, A. Gaita-Arino, E. Coronado and D. Loss, *Nat. Nanotechnol.*, 2007, **2**, 312.
8 M. P. Santoni, G. S. Hanan and B. Hasenknopf, *Coord. Chem. Rev.*, 2014, **281**, 64.
9 C. L. Zhou, S. Li, W. Zhu, H. J. Pang and H. Y. Ma, *Electrochim. Acta*, 2013, **113**, 454.
10 M. Carrar and S. Gross, *Materials*, 2014, **7**, 3956.
11 L. H. Bi, W. H. Zhou, J. G. Jiang and S. J. Dong, *J. Electroanal. Chem.*, 2008, **624**, 269.
12 Y. F. Song and R. Tsunashima, *Chem. Soc. Rev.*, 2012, **41**, 7384.
13 P. Mialane, G. J. Zhang, I. M. Mbomekalle, P. Yu, J. D. Compain, A. Dolbecq, J. Marrot, F. Secheresse, B. Keita and L. Nadjo, *Chem. – Eur. J.*, 2010, **16**, 5572.
14 L. H. Jin, Y. X. Fang, P. Hu, Y. L. Zhai, E. K. Wang and S. J. Dong, *Chem. Commun.*, 2012, **48**, 2101.
15 Z. L. Wang, R. L. Zhang, Y. Ma, A. D. Peng, H. B. Fu and J. N. Yao, *J. Mater. Chem.*, 2010, **20**, 271.
16 (*a*) B. Wang, R. Q. Meng, L. H. Bi and L. X. Wu, *Dalton Trans.*, 2011, **40**, 5298; (*b*) S. Y. Tao, P. Fan, Y. C. Wang, C. Wang, T. Hu and C. G. Meng, *J. Mater. Chem. C*, 2014, **2**, 1962.
17 B. K. Gupta, G. Kedawat, P. Kumar, M. A. Rafiee, P. Tyagi, R. Srivastava and P. M. Ajayan, *J. Mater. Chem. C*, 2015, **3**, 2568.
18 Y. Liu, L. N. Sun, J. L. Liu, Y. X. Peng, X. Q. Ge, L. Y. Shi and W. Huang, *Dalton Trans.*, 2015, **44**, 237.
19 (*a*) G. Mallesham, C. Swetha, S. Niveditha, M. E. Mohanty, N. J. Babu, A. Kumar, K. Bhanuprakash and V. J. Rao, *J. Mater. Chem. C*, 2015, **3**, 1208; (*b*) A. Beneduci, S. Cospito, M. L. Deda and G. Chidichimo, *Adv. Funct. Mater.*, 2015, **25**, 1240.
20 M. R. Rao, C. W. Liao, W. L. Su and S. S. Sun, *J. Mater. Chem. C*, 2013, **1**, 5491.
21 S. T. Wang, E. B. Berda, X. F. Lu, X. F. Li, C. Wang and D. M. Chao, *Macromol. Rapid Commun.*, 2013, **34**, 1648.
22 M. Tomasulo, S. Giordani and F. Raymo, *Adv. Funct. Mater.*, 2005, **15**, 787.
23 X. T. Wang, J. Q. Wang, R. Tsunashima, K. Pan, B. Cao and Y. F. Song, *Ind. Eng. Chem. Res.*, 2013, **52**, 2598.
24 (*a*) B. Wang, L. H. Bi and L. X. Wu, *J. Mater. Chem.*, 2011, **21**, 69; (*b*) L. X. Xu, B. Wang, W. M. Gao, L. X. Wu and L. H. Bi, *J. Mater. Chem. C*, 2015, **3**, 1732.
25 (*a*) B. Qin, H. Y. Chen, H. Liang, L. Fu, X. F. Liu, X. H. Qiu, S. Q. Liu, R. Song and Z. Y. Tang, *J. Am. Chem. Soc.*, 2010, **132**, 2886.
26 H. X. Gu, L. H. Bi, Y. Fu, N. Wang, S. Q. Liu and Z. Y. Tang, *Chem. Sci.*, 2013, **4**, 4371.
27 B. Wang, Z. D. Yin, L. H. Bi and L. X. Wu, *Chem. Commun.*, 2010, **46**, 7163.
28 B. Wang, Y. Y. Ma, S. Wang, L. Y. Zhang, J. Liang, H. L. Li, L. X. Wu and L. H. Bi, *J. Mater. Chem. C*, 2014, **2**, 4423.
29 M. H. Alizadeh, S. P. Harmalker, Y. Jeannin, J. Martin-Frere and M. T. Pope, *J. Am. Chem. Soc.*, 1985, **107**, 2662.
30 G. W. Lu and G. Q. Shi, *J. Electroanal. Chem.*, 2006, **586**, 154.